Biochimica et Biophysica Acta 1788 (2009) 708–716

Contents lists available at ScienceDirect

Biochimica et Biophysica Acta

journal homepage: www.elsevier.com/locate/bbamem

Study of bradykinin conformation in the presence of model membrane by Nuclear Magnetic Resonance and molecular modelling

Claudia Bonechi [a,*], Sandra Ristori [b], Giacomo Martini [b], Silvia Martini [a], Claudio Rossi [a]

[a] Department of Chemical and Biosystem Sciences and CSGI, University of Siena, Via A. Moro 2, 53100 Siena, Italy
[b] Department of Chemistry and CSGI, University of Florence, Via della Lastruccia 3, 50019 Sesto F.no, Florence, Italy

ARTICLE INFO

Article history:
Received 24 September 2008
Received in revised form 29 December 2008
Accepted 31 December 2008
Available online 20 January 2009

Keywords:
Bradykinin
Monolamellar liposome
NMR
DOPC/DOPE

ABSTRACT

The conformation of bradykinin (BK), Arg1-Pro2-Pro3-Gly4-Phe5-Ser6-Pro7-Phe8-Arg9, was investigated by Nuclear Magnetic Resonance (NMR) spectroscopy and Monte Carlo simulation in two different media, i.e. in pure aqueous solution and in the presence of phospholipid vesicles. Monolamellar liposomes are a good model for biological membranes and mimic the environment experienced by bradykinin when interacting with G-protein coupled receptors (GPCRs). The NMR spectra showed that lipid bilayers induced a secondary structure in the otherwise inherently flexible peptide. The results of ensemble calculations revealed conformational changes occurring rapidly on the NMR time scale and allowed for the identification of different families of conformations that were averaged to reproduce the NMR observables. These structural results supported the hypothesis of the central role played by the peptide C-terminal domain in biological environments, and provided an explanation for the different biological behaviours observed for bradykinin.

1. Introduction

Bradykinin (BK; Arg1-Pro2-Pro3-Gly4-Phe5-Ser6-Pro7-Phe8-Arg9) is a nonapeptide hormone produced by enzymatic cleavage of its high molecular weight precursor, kininogen, at the occurrence of tissue injury or trauma [1,2]. It is one of the most potent vasodilators and increases vascular permeability [3]. BK also elicits contraction of smooth muscles of the respiratory and gastrointestinal tract and of the uterus [4], it is active in the central nervous system, where it initiates pain stimuli and is responsible for the cardinal symptoms of inflammation [5–7].

The conformational analysis of this oligopeptide has been the object of considerable interest, with the aim of gaining insights into possible bioactive conformations and developing a structure–activity relationship [8,9]. The general conclusion of conformational studies in aqueous solution is that BK exists in random-coil conformational states [10,11]. BK undergoes conformational modifications and assumes a possible bioactive tertiary structure, when complexed to its receptor [12–14], in the presence of short chain lipids [15], or when interacting with micellar systems [16–20]. The receptor of BK belongs to the family of G-protein-coupled receptors, characterized by seven transmembrane hydrophobic helical segments [21]. A membrane-bound pathway for the interaction between peptide hormones and their receptors has been proposed [22]. This implies accumulation and orientation of the peptide on the membrane surface, which increases the local concentration of BK and at the same time reduces the degrees of its rotational and translational freedom. Such mechanism may also facilitate the transition from the random coil structure, usually adopted by peptides in the extracellular environment, to the bioactive conformation [23].

Unilamellar liposomes are good mimetics of cell membranes, since bilayers are the basic assembly shared by these systems [24,25]. Indeed, monolamellar liposomes present more realistic features than other amphiphilic aggregates.

The main purpose of the present study was to investigate the conformational modifications induced by membrane-like systems (dioleoylphospholipid vesicles) on bradykinin molecules by combining high resolution NMR and computational techniques [26–28]. This represents a suitable approach to determine the structure of biologically relevant molecules in different media [29–32]. Previous studies by electron spin resonance [33] and time-resolved fluorescence [34] spectroscopies of labels intercalated in lipid bilayers have shown that BK and some of its fragments interact with anionic vesicles of dimyristoylphosphatidylglycerol, with significant modification of the bilayer fluidity.

In this work, vesicles were formed with 1,2-dioleoyl-sn-glycero-phosphocholine (DOPC), and 1,2-dioleoyl-sn-glycerophospho-ethanolamine (DOPE), which are commonly used to model plasma membranes, since they give a fluid bilayer at room temperature and since phosphocholine and phosphoethanolamine are the most abundant polar head types found in the outer cell membrane [35]. A comparison was also made with liposomes whose bilayer contained a negatively charged lipid (1,2-dioleoyl-sn-glycero-3-phosphate monosodium salt, DOPA), in order to reproduce the surface of different cell types.

* Corresponding author. Tel.: +39 0577 234372; fax: +39 0577 234177.
E-mail address: cbonechi@unisi.it (C. Bonechi).

0005-2736/$ – see front matter © 2009 Elsevier B.V. All rights reserved.
doi:10.1016/j.bbamem.2008.12.019

Liposomes were characterized by Photon Correlation Spectroscopy and Zeta Potential, to monitor possible changes in the structure and surface charge after association with BK molecules.

The obtained results suggested that the biological activity of bradykinin could be correlated with its interaction with phospholipid bilayers, and supported the hypothesis of an active role of the membrane as a promoter of ligand–receptor interaction.

2. Materials and methods

1,2-dioleoyl-sn-glycero-3-phosphocholine, DOPC (purity>99%), 1,2-dioleoyl-sn-glycero-3-phosphoethanolamine, DOPE (purity>99%) and 1,2-Dioleoyl-*sn*-Glycero-3-Phosphate, DOPA were purchased from Avanti Polar Lipids, Inc., Alabaster, AL, and used without further purification. All liposomes were prepared with a total lipid concentration of 1×10^{-2} M in H_2O or D_2O. The structure and numbering of DOPC and DOPE lipids are shown in Fig. 1.

Bradykinin, Arg1-Pro2-Pro3-Gly4-Phe5-Ser6-Pro7-Phe8-Arg9, (purity≥98%) was obtained from Sigma Aldrich, Milano Italy, and used without further purification.

2.1. Sample preparation and characterization

Three different liposomes were used in this work: DOPC/DOPE (1:1), DOPE/DOPA (1:1) and DOPC/DOPA/DOPE (0.25:0.75:1).

Unilamellar monodisperse lipid vesicles were prepared in the following manner. Appropriate amounts of DOPC and DOPE stock solution (4×10^{-2} M in $CHCl_3$) and of bradykinin stock solution (1×10^{-2} M in C_2H_5OH) were mixed, dried with a nitrogen stream and kept under vacuum overnight at 303 °K, to remove traces of the organic solvent. The dried films were then dissolved in D_2O.

Upon vortexing, multilamellar vesicles were first obtained. Subsequent treatment with nine freeze/thaw cycles and 27 extrusion passages through polycarbonate filters with 100 nm pore diameter (Mini-Extruder device, Avestin Inc., Canada) allowed obtaining unilamellar vesicles of restricted size distribution.

The size of plain- and BK associated-liposomes was determined by photon correlation spectroscopy (PCS) with a Coulter Sub-Micron Particle Analyzer Model N4SD (Coulter Corporation, Miami, FL, USA). Laser light of 632.8 nm wavelength, scattered by the sample at 90°, was amplified and then analyzed to obtain a correlation function. Unimodal fitting, that assumes a log Gaussian distribution of size and SDP (Size Distribution Processor) fitting, based on the algorithm CONTIN, were used to obtain mean diameter and polydispersity index.

ζ potential measurements were performed with a Coulter DELSA 440 SX apparatus. Home made hemispherical electrodes covered by a thin gold layer were used as the measure cell. ζ curves were recorded at four different scattering angles (8.6°, 17.1°, 25.6° and 34.2°) by using an electromagnetic field of 3 V.

2.2. NMR spectroscopy

NMR spectra of plain and BK loaded liposomes were acquired at 298 °K on a Bruker DRX-600 AVANCE spectrometer (Rheinstetten, Germany), equipped with an xyz gradient unit, and operating at 600.13 MHz for ^{1}H. Two dimensional NOESY spectra (spectral width 8 ppm, number of complex points $F_2=2048$, $F_1=512$) were acquired using mixing times of 200 and 400 ms and FID's were processed applied exponential multiple function. Water suppression for the 2D spectra was performed using the presaturation sequence.

Data were processed with the NMRpipe [36] software (3.3 version), and 2D spectra were analyzed with the SPARKY software (3.1 version) by T.D. Goddard and D.G. Kneller, University of California, San Francisco.

Constraint distances were generated with the MARDIGRAS algorithm [28], which uses a complete relaxation matrix approach and assumes overall isotropic molecular motion. As starting model for MARDIGRAS calculations, the final structures of a preliminary unrestrained molecular dynamics and subsequent full energy minimization were used.

2.3. Molecular modelling and structure refinement

Molecular dynamics simulations and molecular mechanics calculations were performed with Macromodel 5.0 program [37,38], on Silicon Graphics (SGI, Sunnyvale, CA, USA), INDIGO 2 Solid Impact working under IRIX 6.3 operating system. The force field used was AMBER [39]. Total energy was minimized by block diagonal and full matrix Newton–Raphson minimization without any initial constraints.

The conformational search analysis was performed with the Monte Carlo protocol [40] and the global minimum structure was selected from populated low energy conformers. Experimentally-derived structural constraints were introduced in the calculations. All minimizations were performed by gradient convergence and were continued until the RMS derivative was below 0.01 kJ/Å. A structural test based on the eigenvalues of the second derivative matrix was performed in order to evaluate the presence of local saddle points.

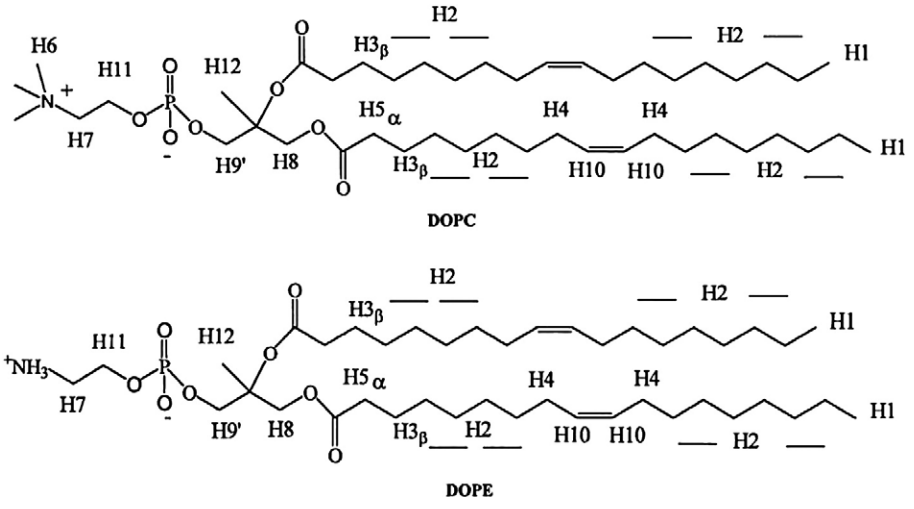

Fig. 1. Structure and numbering of DOPC and DOPE.

In the refinement procedure, the accuracy of the models obtained after molecular dynamics calculations was evaluated on the basis of the XCluster method [41].

3. Results and discussion

Fig. 2 shows the proton spectra recorded at 600 MHz and 298 K for: a) BK ($1.4.10^{-2}$ M) in D_2O solution; b) DOPC/DOPE (1:1) liposome; c) DOPC/DOPE:BK (5:1). Proton signal assignment was based on COSY, TOCSY and NOESY spectra and was in agreement with literature data [42–45] (COSY and TOCSY spectra not shown). In particular, the signals at 7.19 ppm and 7.29 ppm were assigned to aromatic protons (H2,6 and H3,5) for the amino acid Phe5. For the Phe8 the aromatic protons gave resonances at 7.24 ppm (H2,6) and 7.33 ppm (H3,5). The signals at 4.32 ppm and 4.10 ppm were due to the α protons of Arg1 and Arg9, respectively.

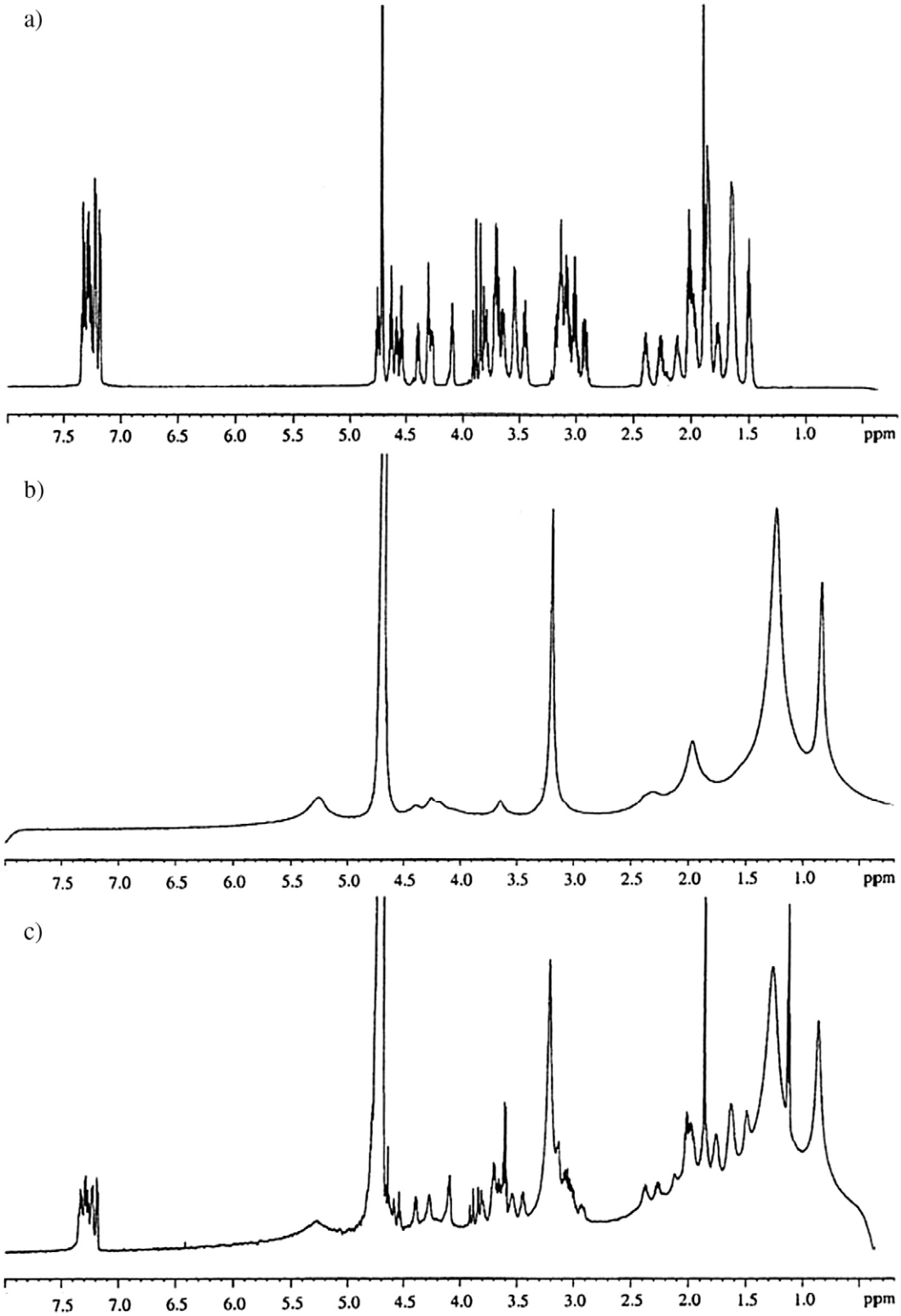

Fig. 2. NMR proton spectra recorded at 600 MHz and 298 K for: (a) BK (1.4×10^{-2} M) in D_2O solution; (b) DOPC/DOPE (1:1) liposome; (c) DOPC/DOPE:BK (5:1).

Table 1
Proton assignments of DOPC/DOPE liposomes

Hn	Chemical shift (ppm)
H_1	0.80
H_2	1.20
$H_{3\beta}$	1.60
$H_{5\alpha}$	2.30
H_4	1.95
H_6	3.20
H_7	3.65
$H_{9'}$	4.25
H_{11}	4.30
H_8	4.40
H_{10}, H_{12}	5.30

Table 2
Inter-residue proton dipolar cross-peaks for BK in D_2O solution obtained by NOESY spectrum

Residue 1	Atom 1	Residue 2	Atom 2
Pro2	Hδ1	Arg1	Hα
Pro2	Hδ2	Arg1	Hα
Pro3	Hδ1	Pro2	Hα
Pro3	Hδ2	Pro2	Hα
Gly4	Hα1	Ser6	Hα
Ser6	Hα	Pro7	Hα
Pro7	Hδ	Ser6	Hα
Pro7	Hβ1	Phe8	H(2,6)
Pro7	Hβ1	Phe8	H(3,5)

The ^1H spectrum of DOPC/DOPE liposomes in D_2O solution (Fig. 2B) showed broad and unresolved signals, which did not allow the determination of proton–proton scalar couplings. As commonly found in this kind of systems, the poor resolution of resonances was a typical characteristic of amphiphilic molecules that form aggregates. It was due both to slow molecular motions and to incompletely averaged dipolar interactions inside the aggregate. In general, NMR studies of peptides incorporated into membranes are extremely difficult, due to drastic line broadening, high concentration of protons in the lipids compared to the embedded peptide, and signal overlap. In our case, however, the choice of monodisperse liposomes with diameters in the range 120–140 nm allowed obtaining of NMR spectra with fairly narrow and well resolved resonances, thus overcoming the main drawbacks of this otherwise powerful method.

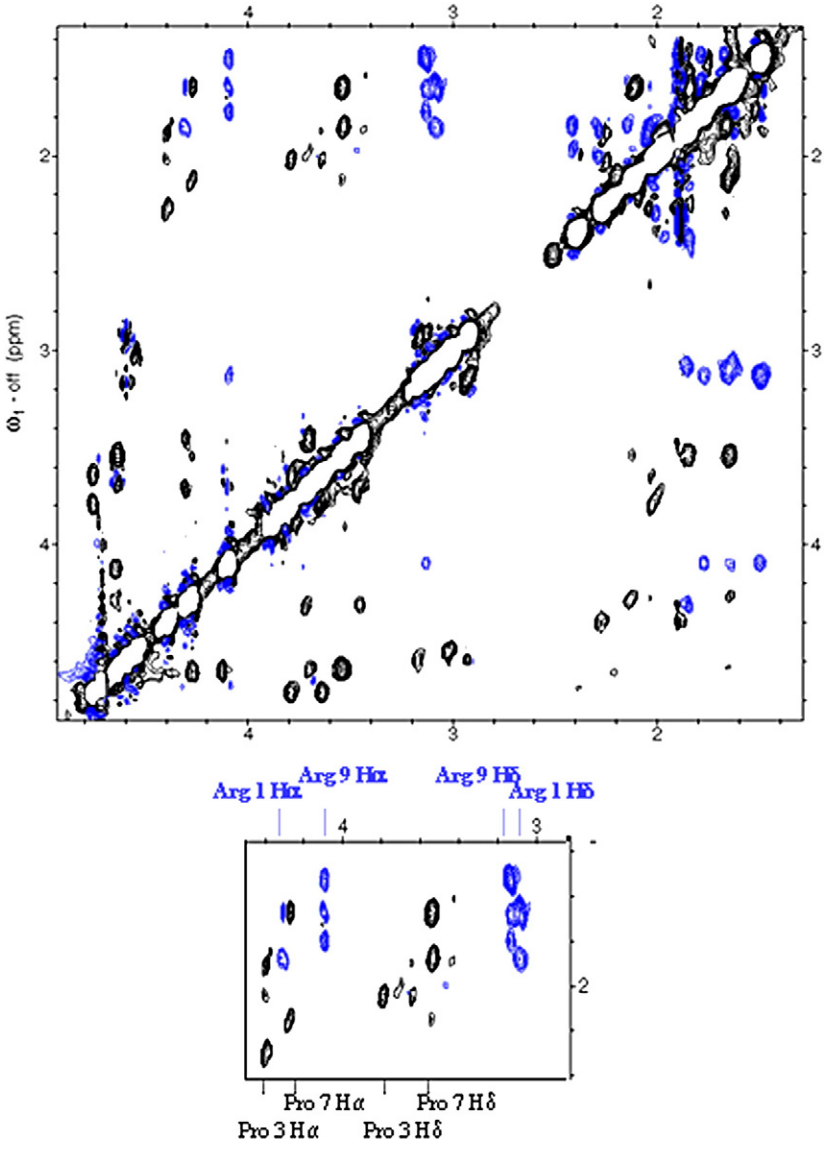

Fig. 3. NOESY spectrum of BK in D_2O solution recorded at 600 MHz, with mixing time of 400 ms. In the insertion the expanded region of α and β, γ, δ protons in the Arg1 and Arg9 amino acids has been reported. In this figure the blue colors refer to the Arg1 and Arg9 cross-peaks which are in the fast motion condition.

Table 3
Intensity of inter-residue cross-peaks for BK in D_2O solution from NOESY spectrum

Residue 1	Atom 1	Residue 2	Atom 2	Intensity	Distance (Å)±0.1
Pro2	Hδ	Arg1	Hα	Strong	2.5
Pro2	Hδ2,1	Arg1	Hα	Strong	2.3
Pro3	Hδ1	Pro2	Hα	Strong	2.2
Pro3	Hδ2	Pro2	Hα	Strong	2.3
Pro7	Hα	Ser6	Hα	Medium	3.3
Gly4	Hα2	Ser6	Hα	Weak	5.0

The assignments of DOPC/DOPE liposomes proton spectrum were reported in Table 1. Fig. 2C shows the ^{1}H spectrum of DOPC/DOPE liposomes containing BK at 1:5 molar ratio with respect to lipids. The NMR resonances of the peptide, in the presence of DOPC/DOPE liposomes, were slightly downfield shifted (−0.034 to −0.040 ppm) with respect to those of BK in aqueous solution. The similarity between the two spectra was attributed to BK exchange between a free state in solution and a membrane-bound state, which caused line broadening of the spectrum without substantially changing the chemical shifts. In the spectrum of Fig. 2C some resonances of BK were still clearly evident, and allowed to study the interaction sites of BK in liposome containing systems. The supposed interaction between BK and liposomes was investigated by NOESY spectra, with the aim of pointing out the differences in the dipolar interactions that occur in aqueous solution and in the presence of liposomes. NOESY experiments are the most useful tool to identify spatial connectivities between nuclei which interact through dipole–dipole couplings, since the size of the NOE is inversely dependent on the distance between interacting spins. The NOESY spectrum of BK in D_2O solution (Fig. 3) showed no indication of an existing secondary structure, since the pattern of NOEs did not reveal any additional significant connectivities. For BK in D_2O solution it was also evident that the cross-peak between Arg1 and Arg9, N-terminal and C-terminal amino acids respectively, showed opposite sign with respect to diagonal peaks (insert of Fig. 3). The relative sign of cross-peaks in a NOESY spectrum depends on the rotational correlation time, i.e. if the rotational correlation time of the molecules is short, the diagonal and cross-peaks have opposite signs [46]. This result allowed assertion that the terminal amino acids of BK experienced a faster motion with respect to backbone amino acids. Both amino acids (Arg1 and Arg9) showed this behaviour in D_2O solution. Only the observed inter residue dipolar cross-peaks in the NOESY spectrum of BK are reported in Table 2. The NOESY spectrum in water displayed very few inter-residue cross-peaks, mainly the αHi and $\delta CH_2(i+1)$. Cross-peaks between Arg1 αH-Pro2 δCH_2 and Pro2 αHPro3 δCH_2 suggested a *trans* conformation for the two proline residues. In fact, the *cis* form would induce much closer contacts between αHi and $\alpha H(i+1)$, whereas the *trans* form promotes short distances between αHi and $\delta CH_2(i+1)$ [47]. It may be noted that native BK was also found in a *trans* arrangement of proline residue in water [47].

Lack of NMR experimental data attributable to secondary structure, made it difficult to define the structural motif of a preferential conformation.

Geometrical restraints were derived from the cross-peak volumes of NOESY spectrum, classifying semi-quantitatively distances into three categories: weak (d=3.7–5.0 Å), medium (d=2.5–3.7 Å) and strong (d=1.8–2.5 Å) [47].

These data were used for theoretical simulations of molecular mechanics and/or molecular dynamics. Here, the procedure involved the following steps: (i) calculation of ^{1}H–^{1}H distances from NOESY intensities by complete relaxation matrix analysis using MARDIGRAS program; (ii) application of restrained molecular mechanics, using a Monte Carlo (MC) [48] approach for sampling the conformational space or molecular dynamic simulations; (iii) statistical analysis of the pool of conformers obtained by the MC simulation, using the program XCluster [49]; (iv) comparison of the free bradykinin conformation and conformational modification in the presence of DOPC/DOPE vesicles.

The NOESY peak volumes were obtained with the Sparky software and used as input values in the MARDIGRAS program. The calculated inter-residue network for BK is reported in Table 3. These proton–proton distances were used as restraints in the Monte Carlo (MC) simulation. Monte Carlo simulations have been demonstrated to be an important tool in the investigation of peptide-membrane interactions [50,51]. We followed a standard MC protocol to sample the conformational space of the peptide in the aqueous phase, using the inter-residue restraints reported in Table 3, and the intra-residue correlation. The acceptance of each step, which creates a new conformation from the previous one, was based on the Metropolis criterion [51] and the internal energy difference between the new and the old state. In the MC protocol, a total of 159 structures of low energy were calculated with an energy global minimum of −1042 kJ/mol and other local energy minima in the range of 4.18, 8.37, 12.55, 20.92, and 41.84 kJ/mol with respect to the absolute minimum.

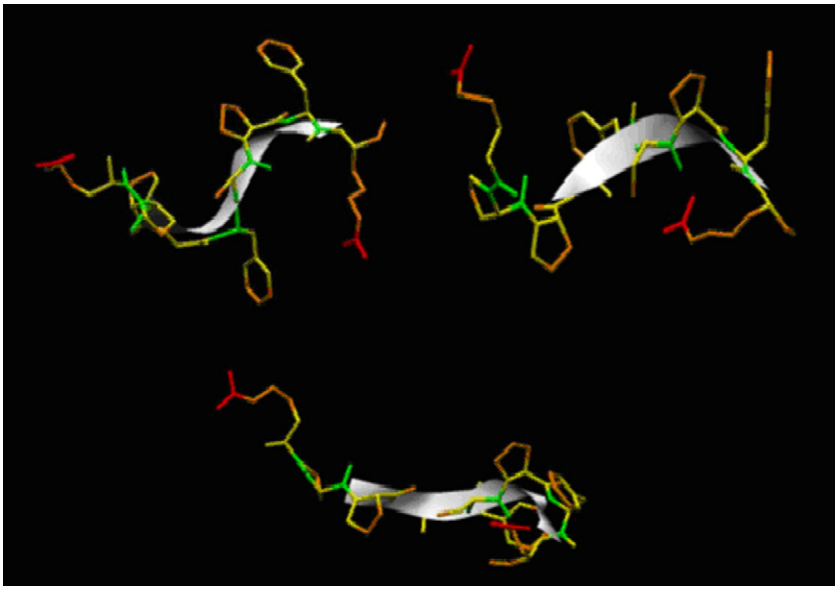

Fig. 4. Three families of conformation for BK having the best agreement with the NOESY distance constraints after the clusters procedure.

The XCluster protocol allowed discarding of the molecules with relative violations of the distance restraint above 1.2–1.5 Å. Thus, we obtained 60 families of conformations. These conformational families represented a structure of bradykinin in aqueous solution only if taken as a whole. In order to calculate the probability of existence of the obtained conformational families, the number of constraints which were respected, was checked. This ensemble of conformations includes all possible secondary structures for the C-terminus of bradykinin. In particular, the first group of families was the one observed from the type I β-turn. A second group of structure clustered around dihedral angle values of a distorted type II β-turn. A third family was intermediate between the two previous ones, and produced a structure that was partially extended instead of being bent. The turn region of representative structures, taken from the three families of conformations obtained from the ensemble calculations, is shown in Fig. 4. This experimental evidence resembled the behaviour of peptides in the presence of receptors. Indeed, bradykinin adopts an active form in solution, when interacting with its receptor.

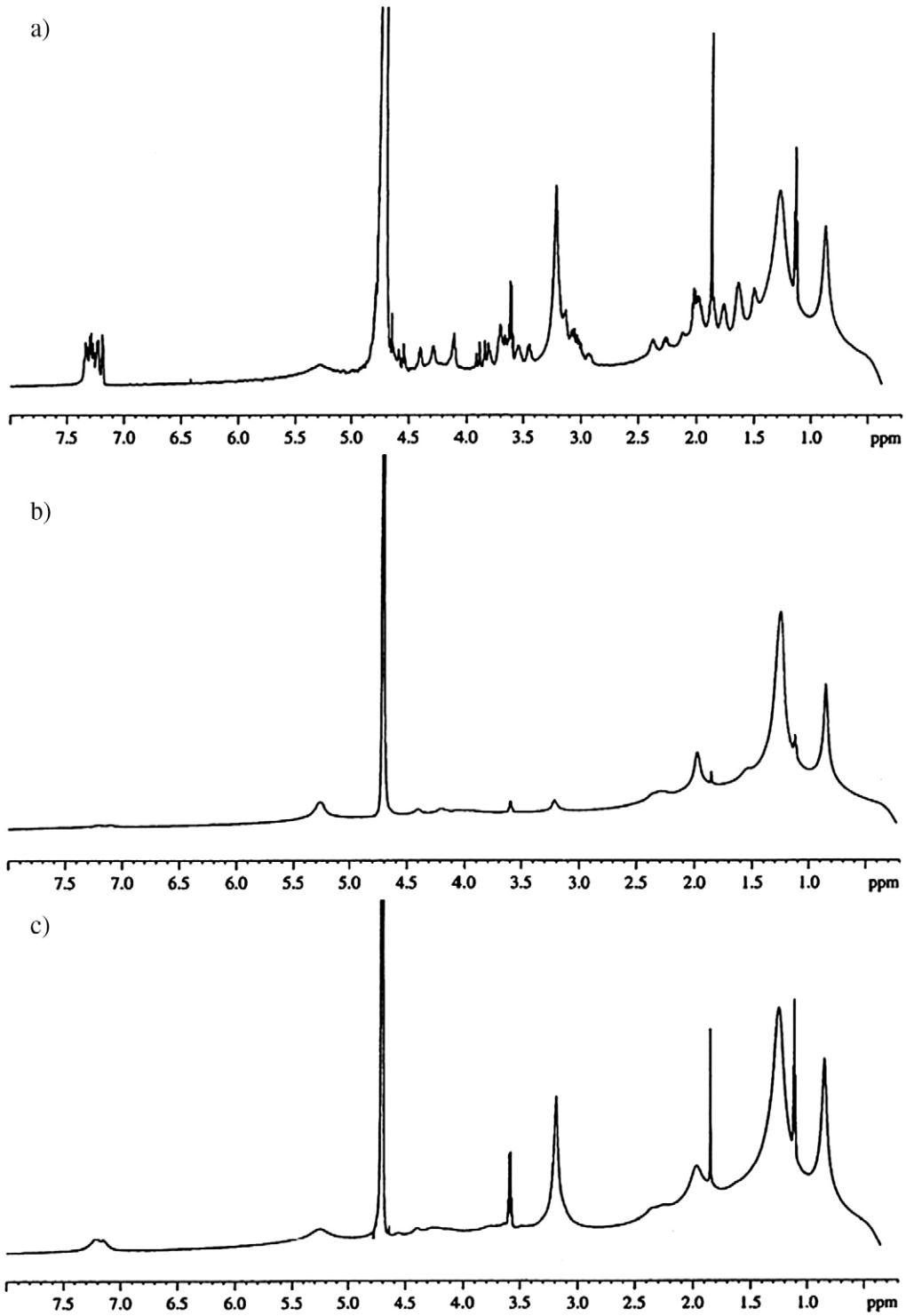

Fig. 5. NMR proton spectra recorded at 600 MHz and 298 K for: (a) DOPC/DOPE:BK (5:1); (b) DOPE/DOPA:BK (5:1); (c) DOPC/DOPA/DOPE:BK (5:1).

Table 4
Size and surface charge of liposomes in pure water and in the presence of BK (1:5 molar ratio with respect to total lipids = 1×10^{-2} M)

Sample composition	Mean diameter (D, nm)	Polyd. index	$D_{95\%}$ (nm) of size distribution	ξ (mV)
DOPC/DOPE (1/1)	125	0.15	122–129	−20±5
DOPC/DOPE (1/1)+BK	140	0.14	139–144	+4±5
DOPC/DOPA/DOPE (0.25/0.75/1)	133	0.12	130–135	−29±2
DOPC/DOPA/DOPE (0.25/0.75/1)+BK	128	0.09	125–130	−10±5
DOPA/DOPE (1/1)	129	0.17	125–133	−37±2
DOPA/DOPE (1/1)+BK	120	0.11	117–123	0±2

In the forth column the width of the diameter distribution is reported for the 95% of total aggregate population.

Table 5
Intensity of cross-peaks for DOPC/DOPE:BK (5:1) from NOESY spectrum

Residue 1	Atom 1	Residue 2	Atom 2	Intensity	Distance (Å)±0.1
Pro3	Hδ2	Pro2	Hα	Strong	2.4
Phe5	Hβ	Phe5	H(2,6)	Strong	2.5
Phe8	Hα	Phe8	H(3,5)	Medium	3.0
Phe8	H(2,6)	Pro7	Hβ1	Weak	4.0
Phe8	H(3,5)	Pro7	Hβ1	Weak	4.1
Phe5	Hβ	Phe5	H(3,5)	Weak	4.3
Phe8	Hβ1	Phe8	H(3,5)	Weak	4.6
Phe8	Hβ2	Phe8	H(3,5)	Weak	4.6

Therefore, membrane binding could be the first step of a membrane-bound activation pathway. This has also been proposed for a number of peptides and receptors [52–55].

As mentioned above, mono and bidimensional NMR experiments were also performed for liposomes containing the negative lipid DOPA, which is a constituent of many bacterial membranes. Bilayers made up with DOPE and DOPA at 1/1 molar ratio and with DOPC, DOPA and DOPE at 0.75/0.25/1 molar ratio were investigated, either in the form of BK free systems or in the presence of bradykinin 5:1 mol: mol with respect to total lipids. The corresponding proton NMR spectra are reported in Fig. 5. By comparing Fig. 5A–C, it could be observed that only the system DOPC/DOPE:BK gave a spectrum in which BK proton resonances were observable. In the two other systems, BK signals disappeared, in particular those of the phenylalanine aromatic protons (7–8 ppm). These evidences suggested that in DOPE/DOPA:BK and DOPC/DOPA/DOPE:BK systems, the peptide completely adhered on the liposome surface, preventing the observation of BK NMR signals. Indeed, the DOPE/DOPA and DOPC/DOPA/DOPE liposomes have a strongly negative surface charge (−37 mV±2 and −29 mV±2 respectively), which is in agreement with the observed strong interaction. A similar behaviour is reported by Marcotte et al. [55] for a pentapetide of the enkephalin family, whose interaction with model membrane (PC and PG bicelles) depends on the nature of

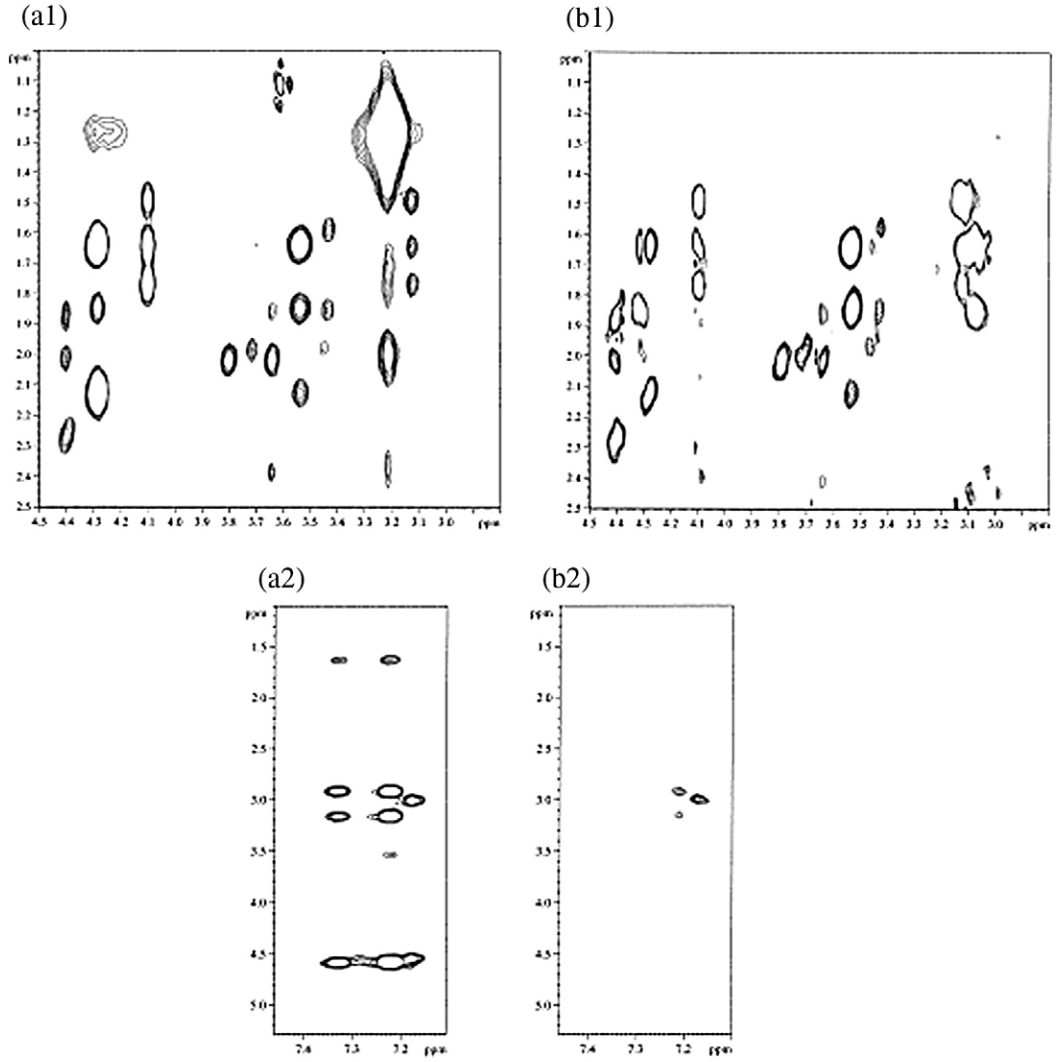

Fig. 6. Two-dimensional NOESY strips, in two different regions, from 600 MHz and 400 ms mixing time for: (a) DOPC/DOPE:BK (5:1); (b) BK in D_2O solution.

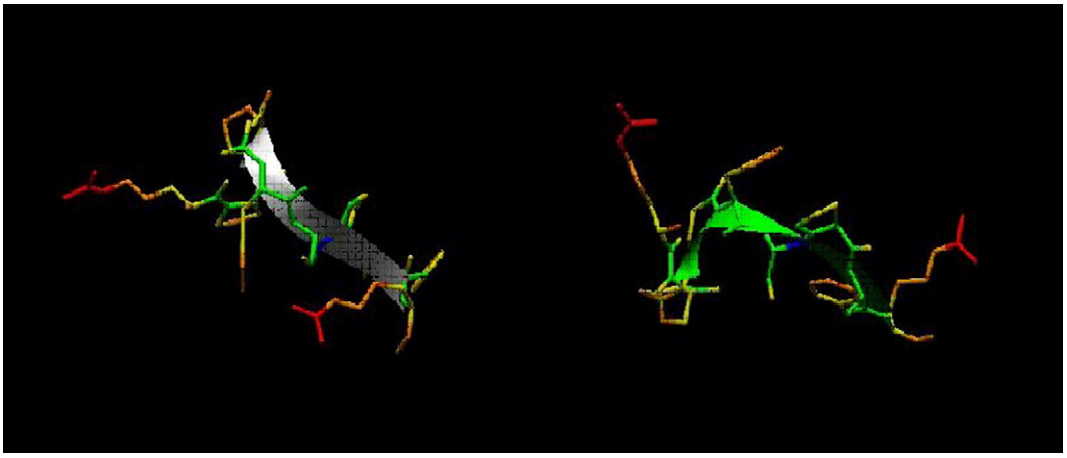

Fig. 7. Only two conformational families for BK in DOPC/DOPE vesicles, obtained by XCluster procedure.

phospholipid headgroups. Table 4 reports the mean size and the surface charge of plain and BK interacting liposomes for the three different bilayer types studied in this work. Data indicated that vesicles diameter did not change substantially after bradykinin addition. The low polydispersity indexes measured for all the systems showed that liposomes were not deeply altered upon interaction with this peptide and remained fairly monodisperse. These features were found to be reproducible and did not change at different liposome concentrations (dilution of the whole system was performed up to 20 times the starting value of 1×10^{-2} M total lipids).

In order to study the conformational modification of BK in the DOPC/DOPE:BK (5:1) system more in detail, the NOESY spectrum of the peptide plus vesicles system was analyzed (Fig. 6A) and compared to the NOESY spectrum of BK without vesicles (Fig. 6B). The NOESY spectrum of DOPC/DOPE:BK (5:1) system displayed some correlations, indicating the adoption of a BK preferred conformation upon interaction with DOPC/DOPE vesicles. The cross-peaks were also broadened with respect to those of BK without lipids, indicating that the peptide underwent slower tumbling as a result of the binding process.

The comparison of NOESY spectra is also important to underline the difference between DOPC/DOPE:BK (5:1) and BK in D_2O solution. The first important evidence concerned the sign of amino acids Arg1 and Arg9 cross-peaks. Contrarily to the results for BK without vesicles, the cross-peaks of Arg1 and Arg9 Hα and Hδ showed the same sign of diagonal peaks for the DOPC/DOPE:BK (5:1) (Fig. 6(a1)). This suggested the existence of a slow motion regime for the two amino acids. We thus concluded that the terminal amino acids did not show a different motional regime with respect to the backbone, and that BK molecules were associated with slowly tumbling large aggregates.

The dipolar cross-peaks for the DOPC/DOPE:BK system are reported in Table 5. Noteworthy: (i) some inter-residue cross-peaks observed in the liposome free systems were no longer present and (ii) the dipolar interactions between aromatic protons of Phe5 and Phe8 appeared (Fig. 6(a2)). These experimental data confirmed that the peptide molecule strongly interacted with liposomes, which induced a preferential secondary structure. In particular, in the NOESY spectrum of the DOPC/DOPE:BK system (Fig. 6(a1)), the cross-peaks Arg1 Hγ–Hδ (1.65–3.08 ppm) and Arg1 Hβ –Hδ (1.65–3.08 ppm) were absent, while the same cross-peaks for the Arg9 were present. Therefore, we concluded that in the DOPC/DOPE:BK system the Arg1 residue was directly involved in the interaction with the surface of liposomes.

The intensities of these cross-peaks were converted into distances using the MARDIGRAS software and the obtained structural information was used as constraints in the Monte Carlo procedure. The MC protocol allowed obtaining of a total of 108 low energy structures, with an energy global minimum of −1086 kJ/mol. As reported above, the XCluster analysis allowed definition of 9 families of structures, where the experimental restraints were fully respected. Indeed, this amino acid showed an optimal conformation to interact with surface of liposome, whereas the Arg1 was not involved in intramolecular interactions. As reported in Fig. 7, two clusters show a predominant conformation for the N-terminal amino acid.

The interaction between DOPC/DOPE phospholipids and bradykinin is driven by the phosphate groups, oriented toward the liposome outer surface (as suggested by the negative ζ potential values of BK free liposomes), which is able to induce the rearrangement of the Arg1 residue.

4. Conclusions

Small peptides, like bradykinin, do not have a single stable conformation in solution. The conformation responsible for their biological behaviour is adopted only at the active site, and also in this case the flexibility of the biomolecule determines the mechanism of action. In this study, we showed that BK molecules interact with zwitterionic lamellar systems and that the amino acid Arg1 is directly involved in this process, possibly in tight contact with the polar head groups. Therefore, Arg1 acts as a tethering point between the peptide and the membrane surface. The central portion of the amino acid sequence (Pro2-Pro3-Gly4-Phe5), may contribute to anchor the peptide to the membrane environment and to maintain the N- and C-termini amino acids in the optimal topological orientation. Overall, the interaction with the membrane surface provided the topological arrangement of the biologically important ligand regions. Moreover, it was found that the aromatic amino acids (Phe5 and Phe8) also showed a preferential conformation in the presence of liposome.

In conclusion, this study supports the idea that membranes play a crucial role in inducing and stabilizing the structures of peptide hormones.

Acknowledgements

The authors thank the University of Siena for financial support.

References

[1] S.G. Farmer, R.M. Burch, in: R.M. Burch (Ed.), In Bradykinin Antagonists, Basic and Clinical Research, Marcel Dekker, New York, 1991, pp. 1–31.
[2] M.E. Moreau, N. Garbacki, G. Molinaro, N.J. Brown, F. Marceau, A. Adam, The kallikrein–kinin system: current and future pharmacological targets, J. Pharmacol. Sci. 99 (1) (2005) 6–38.
[3] L.F. Carbonell, O.A. Carretero, J.M. Stewart, A.G. Scicli, Effect of a kinin antagonist on the acute antihypertensive activity of enalaprilat in severe hypertension, Hypertension 11 (1988) 239–243.

[4] D. Ragoli, J. Barabe, Pharmacology of bradykinin and related kinins, Pharmacol. Rev. 32 (1980) 1–46.
[5] A. Dray, M. Perkins, Bradykinin and inflammatory pain, Trends Neurosci. 16 (1993) 99–104.
[6] D.J. Kyle, R.M. Burch, A survey of bradykinin receptors and their antagonists, Curr. Opin. Invest. Drugs 2 (1) (1993) 5–20.
[7] M. Miskolzie, L. Gera, J.M. Stewart, G. Kotovych, Correlation of secondary structures of bradykinin B1 receptor antagonists with their activity, J. Biomol. Struct. Dyn. 19 (2002) 585–593.
[8] P. Desai, E. Coutinho, S. Srivastava, Conformational diversity of T-kinin in DMSO, water and HFA, Eur. J. Med. Chem. 37 (2002) 135–146.
[9] J. Jensen, A.M. Soto, J.M. Colon, Structure–activity relationships of trout bradykinin ([Arg0,Trp5,Leu8]-bradykinin), Peptides 21 (2000) 1793–1798.
[10] X. Cai, C. Dass, Conformational analysis of proteins and peptides, Current Organic Chemistry 7 (18) (2003) 1841–1854 (14).
[11] D.J. Kyle, J. A Martin, S.G. Farmer, R.M. Burch, Design and conformational analysis of several highly potent bradykinin receptor antagonists, J. Med. Chem. 34 (1991) 1230–1233.
[12] D.G. Sawutz, J.M. Salvino, P.R. Seoane, B.D. Douty, W.T. Houck, M.A. Bobko, M.S. Doleman, R.E. Dolle, H.R. Wolfe, Synthesis, characterization, and conformational analysis of the D/L-Tic7 stereoisomers of bradykinin receptor antagonist DArg0 [Hyp3,Thi5,D-Tic7,Oic8]bradykinin, Biochemistry 33 (9) (1994) 2373–2379.
[13] H. Ottleben, M. Haasemann, R. Ramachandran, M. Görlach, W. Müller-Esterl, L.R. Brown, An NMR study of the interaction of 15N-labelled bradykinin with an antibody mimic of the bradykinin B2 receptor, Eur. J. Biochem. 244 (1997) 471–478.
[14] G. Kotovych, J.R. Cann, J.M. Stewart, H. Yamamoto, NMR and CD conformational studies of bradykinin and its agonists and antagonists: application to receptor binding, Biochem. Cell Biol. 76 (2–3) (1998) 257–266.
[15] L. Denys, A.A. Bothner-By, G. Fisher, Conformational diversity of bradykinin in aqueous solution, Biochemistry 21 (1982) 6531–6536.
[16] C. Chatterjee, C. Mukhopadhyay, Conformational alteration of bradykinin in presence of GM1 micelle, Biochem. and Biophys Res. Communications 315 (4) (2004) 866–871.
[17] R.S. Prosser, F. Evanics, J.L. Litevski, M. Sameer Al-Abdul-Wahid, Current applications of bicelles in NMR studies of membrane-associated amphiphiles and proteins, Biochemistry 45 (28) (2006) 8453–8465.
[18] J.R. Cann, A. Vatter, R.J. Vavrek, J.M. Stewart, Interaction of bradykinin with sodium dodecyl sulfate and certain acidic lipids, Peptides 7 (1986) 1121–1130.
[19] M. Pellegrini, S. Mammi, E. Peggion, D.F. Mierke, Threonine6-bradykinin: structural characterization in the presence of micelles by nuclear magnetic resonance and distance geometry, J. Med. Chem. 40 (1997) 92–98.
[20] S.I. Hakomari, Structure & function of sphingoglycolipids in transmembrane signaling and cell–cell interaction, Biochem. Soc. Trans. 21 (1993) 583–585.
[21] A.D. Strosberg, C. Nahmias, G-protein-coupled receptor signalling through protein networks, Biochem. Soc. Trans. 35 (2007) 23–27.
[22] L. Moroder, R. Romano, W. Guba, D.F. Mierke, H. Kessler, C. Delporte, J. Winand, J. Christophe, New evidence for a membrane bound pathway in hormone receptor binding, Biochemistry 32 (1993) 13551–13559.
[23] R. Schwyzer, Peptide-membrane interactions and a new principle in quantitative structure–activity relationships, Biopolymers 31 (1991) 785–792.
[24] A.S. Ulrich, Biophysical aspects of using liposomes as delivery vehicles, Biosci. Rep. 22 (2) (2002) 129–150.
[25] K. Lohner, E. Sevcsik, G. Pabst, Liposome-based biomembrane mimetic systems: implications for lipid–peptide interactions, Advances in Planar Lipid Bilayers and Liposome 6 (2008) 103–137.
[26] L.K. Tamm, L. Binyong, NMR of membrane proteins in solution, Prog. Nucl. Magn. Reson. Spectrosc. 48 (4) (2006) 201–210.
[27] B.A. Borgias, T.L. James, Two-dimensional nuclear Overhauser effect: complete relaxation matrix analysis, Methods Enzymol. 176 (1989) 169–183.
[28] C. Wang, J. Yao, Y. Yu, X. Shao, Y. Cui, H. Liu, L. Lai, R. Wang, Structure–activity study of endomorphin-2 analogs with C-terminal modifications by NMR spectroscopy and molecular modelling, Bioorg. & Med. Chemistry 16 (12) (2008) 6415–6422.
[29] W.R.P. Scott, S.B. Baek, D. Jung, R.E.W. Hancock, S.K. Straus, NMR structural studies of the antibiotic lipopeptide daptomycin in DHPC micelles, Biochim. Biophys. Acta 1768 (2008) 3116–3126.
[30] K. Wakamatsu, A. Takeda, T. Tachi, K. Matsuzaki, Dimer structure of magainin 2 bound to phospholipid vesicles, Biopolymers 64 (2002) 314–327.
[31] Ø. Halskau, N.Å. Frøystein, A. Muga, A. Martínez, The membrane bound conformation of a-lactalbumin studied by NMR-monitored 1H exchange, J. Mol. Biol. 321 (2002) 99–110.
[32] M. Garcia-Fuentes, D. Torres, M. Martin-Pastor, M.J. Alonso, Application of NMR spectroscopy to the characterization of PEG-stabilized lipid nanoparticles, Langmuir 20 (2004) 8839–8845.
[33] R.F. Turchiello, L. Juliano, A.S. Ito, M.T. Lamy-Freund, How bradykinin alters the lipid membrane structure: a spin label comparative study with bradykinin fragments and other cations, Biopolymers 54 (2000) 211–221.
[34] R.F. Turchiello, M.T. Lamy-Freund, I.Y. Hirata, L. Juliano, A.S. Ito, Orthoaminobenzoic acid labeled bradykinins in interaction with lipid vesicles: fluorescence study, Biopolymers 65 (2002) 336–346.
[35] P. Yeagle (Ed.), The Structure of Biological Membranes, CRC Press, Boca Raton, Florida, 2005.
[36] F. Delaglio, S. Grzesiek, G. Vuister, G. Zhu, J. Pfeifer, A. Bax, NMRPipe: a multidimensional spectral processing system based on UNIX pipes, J. Biomol. NMR 6 (1995) 277–293.
[37] C. Still, Macromodel, Columbia University Molecular Modelling System, , 1987.
[38] F. Mohamadi, N.G.J. Richards, W.C. Guida, R. Liskamp, M. Lipton, C. Caufield, G. Chan, T. Hendrickson, W.C. Still, Macromodel—an integrated software system for modeling organic and bioorganic molecules using molecular mechanics, J. Comput. Chem. 11 (1990) 440–467.
[39] A. Case, T.E. Cheatham III, T. Darden, H. Gohlke, R. Luo, K.M. Merz Jr., A. Onufriev, C. Simmerling, B. Wang, R. Woods, The Amber biomolecular simulation programs, J. Computat. Chem. 26 (2005) 1668–1688.
[40] G. Chang, W.C. Guida, W.C. Still, An internal-coordinate Monte Carlo method for searching conformational space, J. Am. Chem. Soc. 11 (1989) 4379–4386.
[41] P.S. Shenkin, D.Q. Mcdonald, Cluster analysis of molecular conformations, J. Comput. Chem. 15 (1994) 899–916.
[42] S.R. Mirmira, S. Durani, S. Srivastava, R.S. Phadke, Occurrence of β-bends in bradykinin dissolved in DMSO-d6, Magn. Res. Chem. 28 (7) (1990) 587–593.
[43] R.E. London, J.M. Stewart, J.R. Cann, N.A. Matwiyoff, 13C and proton nuclear magnetic resonance studies of bradykinin and selected peptide fragments, Biochemistry 17 (1978) 2270–2283.
[44] D. Chapman, S. Chen, Thermal and NMR spectroscopic studies of lipids and membranes, Chem. Phys. Lipids 8 (1972) 318–326.
[45] J.M. Neumann, A. Zachowski, S. Tran-Dinh, P.F. Devaux, High resolution proton magnetic resonance of sonicated phospholipids, Eur. Biophys. J. 11 (1985) 219–233.
[46] M.H. Levitt, Spin Dynamics: Basics of Nuclear Magnetic Resonance, John Wiley & Sons, 2001.
[47] K. Wüthrich, NMR of proteins and Nucleic Acids, John Wiley & Sons, New York, 1986.
[48] M.W. Maddox, M.L. Longo, A Monte Carlo study of peptide insertion into lipid bilayers: equilibrium conformations and insertion mechanisms, Biophys. J. 82 (2002) 244–263.
[49] C. Still, XCluster 1.2, Columbia University, New York, 1995.
[50] L. Lins, B. Charloteaux, A. Thomas, R. Brasseur, Computational study of lipiddestabilizing protein fragments: towards a comprehensive view of tilted peptides, Proteins 44 (2001) 435–447.
[51] N. Metropolis, A.W. Rosenbluth, M.N. Rosenbluth, A.H. Teller, E.J. Teller, Equation of state calculations by fast computing machines, J. Chem. Phys. 21 (1953) 1087–1092.
[52] C. Bissantz, Conformational changes of G-protein coupled receptors during their activation by agonist binding, J. Receptors and Signal Transduction 23 (2 & 3) (2003) 123–153.
[53] G.R. Nakamura, M.E. Reynolds, Y.M. Chen, M.A. Starovasnik, Stable "zeta" peptides that act as potent antagonists of the high-affinity IgE receptor, PNAS 99 (3) (2002) 1303–1308.
[54] X. He, D. Chow, M.M. Martick, K.C. Garcia, Allosteric activation of a spring-loaded natriuretic peptide receptor dimer by hormone, Science 293 (5535) (2001) 1657–1662.
[55] I. Marcotte, F. Separovic, M. Auger, S. Gagné, A multidimensional 1H-NMR investigation of the conformation of Methionine–Enkephalin in fast-tumbling bicelles, Biophys. J. 86 (2004) 1587–1600.